NUCLEAR REACTIONS -- THEORY

IMPACT PARAMETER DEPENDENCE OF PROTON INTERFEROMETRY

C. M. Mader and W. Bauer

The two-proton correlation function provides information on the size and lifetime of the hot reaction zone formed in heavy ion collisions. In most studies, measurements of this two-particle observable proposed by Koonin [1] have been compared to calculations using zero-lifetime Gaussian sources. However, this is only a parameterization of an average source size and provides limited information on the space-time evolution of the collision zone.

Detailed calculations using the microscopic Boltzmann-Uehling-Uhlenbeck (BUU) hadronic transport model are in good agreement not only with single-particle observables, such as proton energy spectra, but also the two-particle correlation functions [2]. Recent experiments have provided more stringent tests of the model. In these experiments, gating on centrality was possible. Once again, both the single- and two-particle observables of the BUU predictions are in agreement with the data [3] allowing a more detailed description of the evolution of the hot nuclear matter formed in the collision.

The correlation function is defined as the ratio of the probability of observing a pair of protons (Π_{12}), one with momentum $\vec{p}_1$ and the other with momentum $\vec{p}_2$, relative to the probability of observing two single protons (Π_i) with momentum $\vec{p}_i$, where $i = 1, 2$. Assuming that final state interactions between the protons and their source are negligable and that the two-proton interactions dominate, the correlation function can be expressed in terms of the total ($\vec{P} = \vec{p}_1 + \vec{p}_2$) and relative ($\vec{q} = \frac{1}{2}(\vec{p}_1 - \vec{p}_2)$) momenta of the particles. The explicit relation is

$$C(\vec{P},\vec{q}) = R(\vec{P},\vec{q}) + 1 = \frac{\Pi_{12}(\vec{p}_1,\vec{p}_2)}{\Pi_1(\vec{p}_1)\Pi_1(\vec{p}_2)} \tag{1}$$

$$= \frac{\int d^4x_1 d^4x_2 g(\frac{1}{2}\vec{P},x_1) g(\frac{1}{2}\vec{P},x_2) |\phi(\vec{q},\vec{r}_1-\vec{r}_2+\frac{\vec{P}(t_2-t_1)}{2m})|^2}{\int d^4x_1 g(\frac{1}{2}\vec{P},x_1) \int d^4x_2 g(\frac{1}{2}\vec{P},x_2)}$$

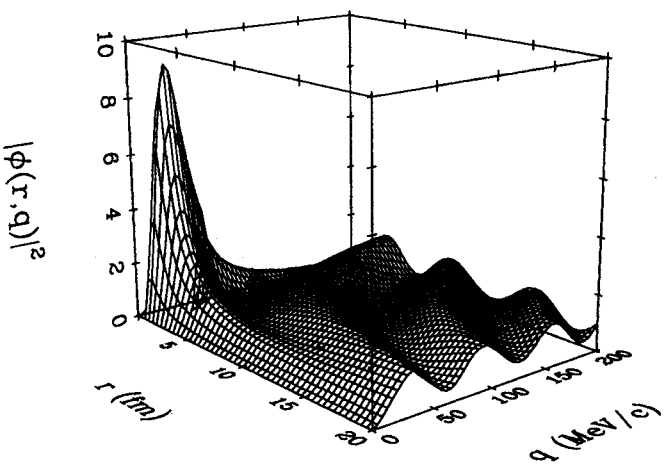

Figure 1: The relative wave function, $|\phi(q, r, cos(\theta))|^2$, for fixed angle $\theta = 45°$ as a function of relative position and momentum. [5]

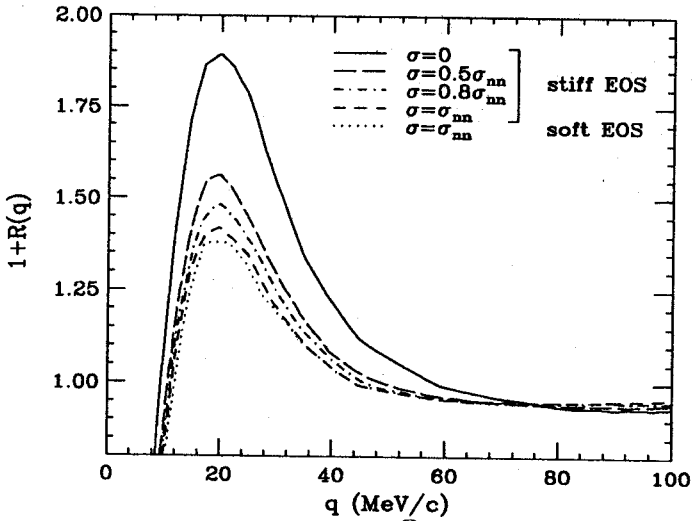

Figure 2: Correlation functions calculated for 75 MeV/A ^{14}N + ^{27}Al at $\langle\theta_{lab}\rangle = 25°$ for $P = 500$ MeV/c. The different lines represent BUU predictions using different values of σ_{nn} and nuclear EoS [2].

where x_i is the proton space-time emission point, $g(\frac{1}{2}\vec{P}, x_i)$ is the phase space distribution, and $\phi(\vec{q}, \vec{r})$ is the two-proton relative wave function [4]. This wave function is shown in figure 1 for two protons at a relative angle of 45°. The wave function vanishes at $r = 0$ due to the Coulomb repulsion of the protons. The strong peak at $q \approx 20$ MeV/c, often referred to as the ^{2}He "resonance", is due to the strong nuclear interaction between the protons. As shown in the correlation functions plotted in figure 2, this peak in the relative wave function leads to an enhancement in the correlation function at $q \approx 20$ MeV/c. The height of this peak is inversely related to the size of the source.

To calculate the correlation functions using equation [1] the single-particle phase space distribution $g(\frac{1}{2}\vec{P}, x_2)$ predicted by BUU is used. The time evolution of the phase space distribution is calculated using the test particle method to solve the BUU equation:

$$\frac{\partial f}{\partial t} + \vec{v} \cdot \nabla_r f - \nabla_r U \cdot \nabla_p f = \frac{4}{(2\pi)^3} \int d^3k_2 d^3k_3 d\Omega v_{12} \frac{d\sigma}{d\Omega} \delta^3(\vec{k}_1 + \vec{k}_2 - \vec{k}_3 - \vec{k}_4) \tag{2}$$

$$\times[(f_1 f_2(1 - f_3)(1 - f_4) - f_3 f_4(1 - f_1)(1 - f_1)].$$

In this model, individual nucleons move in a mean field while experiencing nucleon-nucleon collisions with Pauli blocking of occupied final states [6].

BUU calculations successfully predict single particle observables such as proton energy spectra. In figure 3 we show the transverse energy (E_t) spectra from 80 MeV/A ^{36}Ar + ^{45}Sc collisions where the results of the numerical calculations have been passed through a detector filter. For central events, the BUU results are in good agreement with the data, and for peripheral events the BUU results slightly underpredict the low E_t portion of the spectra.

In these calculations, we have used the in-medium nucleon-nucleon cross section (σ_{nn}) equal to the free value, and a stiff nuclear equation of state (EoS). In figure 2, the effect of changing these two assumptions is shown. Higher values of σ_{nn} increase the number of nucleon-nucleon collisions and since rescattering after hard collisions can only serve to increase the size of the system, the peak at $q \approx 20$ MeV/c decreases, as seen in figure 2. It is not surprising that the difference between using a soft and a stiff nuclear equation of state is much less

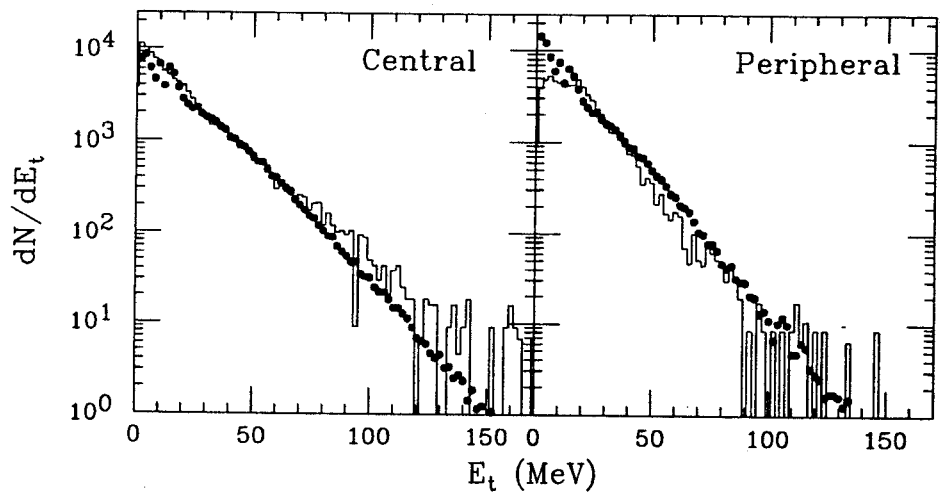

Figure 3: Transverse energy spectra for 80 MeV/A ^{36}Ar + ^{45}Sc at $\langle\theta_{lab}\rangle = 38°$. Data are given by solid symbols. BUU calculation results, filtered for geometrical acceptance, are given by the histograms [7].

pronounced. At the beam energies considered here, the maximum densities reached are not much above nuclear matter density, and compressional effects should play only a minor role. In the work of Gong, *et al.* [2], it was shown that best agreement with the data was obtained with the in-medium σ_{nn} set to the free value and a stiff EoS.

In the more recent experiment of Lisa *et al.* [3], the correlation functions were also gated on centrality. Figure 4 shows both the experimental and theoretical correlation functions for central and peripheral collisions. Once again, the agreement is good, although the peak heights are slightly underpredicted for the peripheral gates. This corresponds to a difference in source radii of about 0.5 fm between calculation and experiment. In figure 5 we show the peak height as a function of total momentum for both central and peripheral collisions. In both central and peripheral events, the BUU predictions reproduce the trend of the data: the peak height increases with increasing total momentum.

Simple parametrizations of the reaction zone can be extracted using Gaussian source parameters. On the right axis in figure 5 we show the apparent source size corresponding to the given peak height extracted using a zero-lifetime Gaussian source. In central collisions, the source size decreases with increasing total momentum of the pair. This implies that the faster protons may be emitted earlier in the collision. The peripheral collisions, are most sensitive to the exact definition of centrality and the differences in the experimental and theoretical curves could be due to the range of impact parameters chosen in the theoretical calculations.

In summary, good agreement with the total momentum and impact parameter dependence of the experimentally measured two-proton correlation function is found, however, the predictions using the BUU phase space distributions generally over-estimate the apparent experimental source size by ≈ 0.5 fm.

References

1. S.E. Koonin, Phys. Lett. **70B**, 43 (1977).
2. W.G. Gong, et. al., Phys. Rev. C **43**, 1804 (1991).
3. M.A. Lisa, et al., submitted to Phys. Rev. C (1993).
4. S. Pratt, Phys. Rev. Lett. **53**, 1219 (1984).
5. W. Bauer, Nucl. Phys. A, **545**, 369c (1992).
6. W. Bauer, Phys. Rev. Lett. **61**, 2534 (1988).
7. M. A. Lisa private communcation.

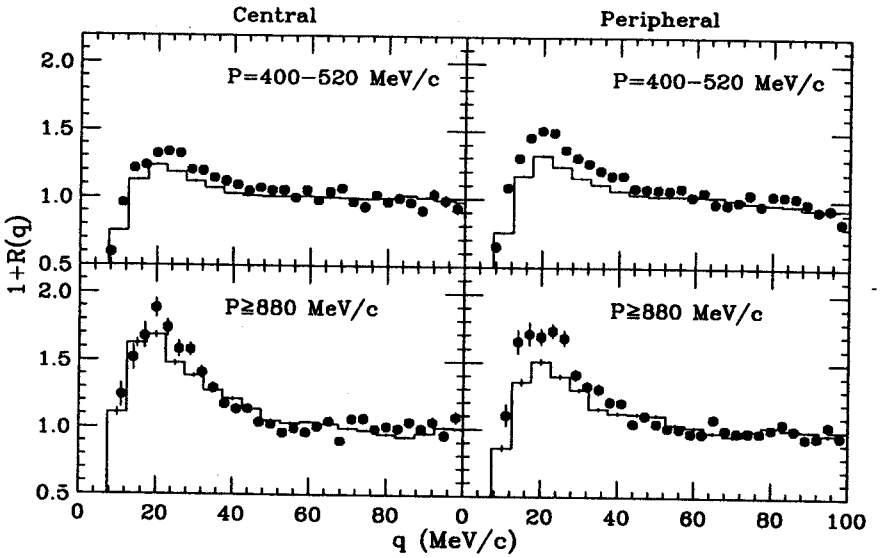

Figure 4: Correlation functions calculated for 80 MeV/A ^{36}Ar + ^{45}Sc at $\langle\theta_{lab}\rangle = 38°$. The solid points represent the experimentally measured correlation functions while the histograms represent correlation functions predicted by BUU [3].

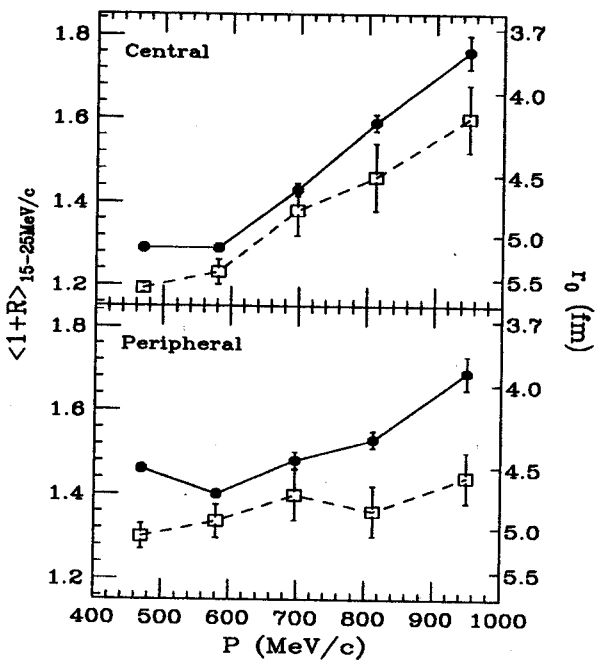

Figure 5: Average peak height of the two-proton correlation function as a function of total momentum for 80 MeV/A ^{36}Ar + ^{45}Sc at $\langle\theta_{lab}\rangle = 38°$. The scale on the right axis is the Gaussian source radius. The solid points represent the experimental correlation functions, open points represent the predictions of BUU [3].

PION CORRELATIONS IN PROTON-INDUCED REACTIONS

C. M. Mader, W. Bauer, P. Danielewicz, D. Klakow[a], and P. Schuck[b]

In nucleon-nucleus collisions at relativistic energies, pions can be used to probe the evolution of the reaction zone. Resonance production and pion absorption play an important role in all observables. However, two-pion correlation functions can provide a great deal of insight into these effects. The $\pi^+\pi^-$ invariant-mass correlation is defined as:

$$R_{\pi^+\pi^-}(M_{inv}) = \frac{\Pi_2(\pi^+\pi^-)}{\Pi_1(\pi^+)\Pi_1(\pi^-)}, \tag{1}$$

where Π_2 is the probability of observing a pair of pions in a single event, and Π_1 is the probability of observing a single pion. Resonant states in the $\pi^+\pi^-$ system would show up as an enhancement at the mass of the resonance. Pluta et. al. [1] have, in fact, seen such an enhancement at $M_{inv}(\pi^+\pi^-)) \approx 2M_\pi$ in p + Pb collisions at 1.6 GeV. However, for light targets, there is no observed enhancement.

We use an extended Boltzmann-Uehling-Uhlenbeck (BUU) hadronic transport model [2] to study the effect of pion absorption and re-scattering on the invariant-mass correlation function. In this model, we propagate protons, neutrons, pions, Delta and N* resonances by numerically solving the BUU equation:

$$\frac{\partial f}{\partial t} + \vec{v}\cdot\nabla_r f - \nabla_r U\cdot\nabla_p f = \frac{4}{(2\pi)^3}\int d^3k_2 d^3k_3 d\Omega v_{12}\frac{d\sigma}{d\Omega}\delta^3(\vec{k}_1+\vec{k}_2-\vec{k}_3-\vec{k}_4) \tag{2}$$

$$\times[f_1 f_2(1-f_3)(1-f_4) - f_3 f_4(1-f_1)(1-f_1)].$$

The particles interact via hadron-hadron collisions where we use the experimentally measured energy-dependent free cross sections where available and evaluate all other cross sections using detailed balance and/or isospin symmetry.[3]

Previous studies using the BUU transport model have shown that absorption and re-scattering of pions in asymmetric nucleus-nucleus collisions at E/A $\approx$ 1 GeV can account for the observed collective pion flow.[4,5] The processes that proved to be most important were:

$$N + N \leftrightarrow N + \Delta \leftrightarrow N + N + \pi. \tag{3}$$

Through these processes, pions were absorbed and re-scattered in the spectator matter and, in non-central collisions focussed into one hemisphere. In figure 1 we demonstate this effect by showing a superposition of 50 non-central p + Pb collisions. The trajectories of pions (thin dots) and resonances (thick dots) are projected onto the reaction plane. While some tracks do scatter toward the center of the target nucleus, most of these pions and resonances rescatter and eventually the resonances all decay and the pions are absorbed. However, the pions and resonances scattered away from the center of the target eventually escape, and thus most of the pions are emitted away from the center. Similar scenarios have been proposed by the WA-80 collaboration to explain observed angular correlations of pion pairs for p + Au collisions at beam energies of 4.9, 60, and 200 GeV.

To check if shadowing by spectator nucleons influences the invariant-mass correlation function, we use the pion pairs predicted by the extended BUU model. At the beam energies considered here, true $\pi^+\pi^-$ pairs are produced in less than 5% of the events. In two pion events, the pions emitted first (π_1) have more kinetic energy available, and the pion spectrum for these particles is not as steep as the spectrum for those which are produced

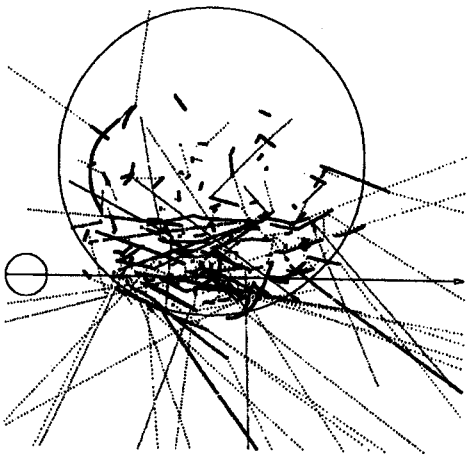

Figure 1: Superposition of pion and delta-resonance tragectories (thin-dots and thick-dots respectively) projected onto the reaction plane for 50 1.6 GeV p + Pb events at b = 5fm.

second (π_2). In order to increase statistics in the numerator but retain the kinematic constraints, we construct all possible $\pi_1^{\pm}\pi_2^{\mp}$ pairs ($N(M_{inv})$) from pions created in two pion events with the same impact parameter and reaction plane.

In order to generate background events in a manner corresponding to the experimentally observed background, we construct all possible $\pi^+\pi^-$ pairs ($N(M_{inv,\phi})$) with random reaction plane orientation and from any impact parameter. The correlation function is then given by

$$R_{\pi^+\pi^-}(M_{inv}) = \frac{\int dbw(b)N(M_{inv},b)}{\int db_1db_2w(b_1,b_2)N(M_{inv,\phi},b_1,b_2)} \tag{4}$$

where the weighting functions ($w(b), w(b_1,b_2)$) take into account the number of real pairs relative to the number of pairs used in our calculations. In

figure 2 we show the calculated correlation functions for the reactions 1.6 GeV p + C and 1.6 GeV p + Pb along with the experimental results. We have normalized the theoretical curves such that $R_{\pi^+\pi^-}(0.5GeV) = 1.0$ and filtered the pions used in the calculation to account for geometrical and energy cuts of the DIOGENE detector. In both the theoretical and experimental results, there is a large enhancement at $M_{inv}(\pi^+\pi^-) = 2M_\pi$ in the lead system, but no enhancement is seen in the carbon system. This is due to the fact that the mean absorption length of the pions is much shorter than the size of the lead nucleus but not the carbon nucleus. This leads to a focussing of the pions all to one side of the reaction plane, creating more true pairs with low invariant-mass while the background pairs (due to randomization of the reaction plane) show no such focussing effects and therefore have no bias toward low mass pairs.

a. Institut für theoretische Physik, Universität Erlangen, Germany.
b. Institut de Physique Nucléaire, Université de Grenoble, France.

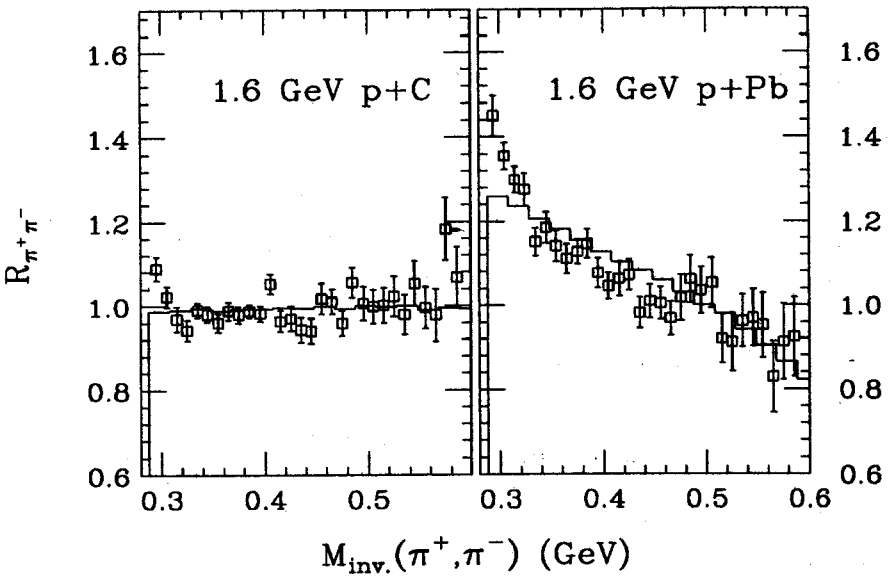

Figure 2: Two pion correlation function as a function of the invariant-mass of the $\pi^+\pi^-$ pair for 1.6 GeV p + C and Pb. The squares are the experimental data of Pluta *et al.* [1] and the histograms are the calculations using the transport model.

References

1. J. Pluta, *et al.* (DIOGENE collaboration), submitted to Nucl. Phys. (1992).
2. B.A. Li and W. Bauer, Phys. Lett. **B254**, 335 (1991); Phys. Rev. C **44**, 450 (1991).
3. P. Danielewicz and G.F. Bertsch, Nucl. Phys. A **533**, 712 (1991).
4. B.A. Li, W. Bauer, and G.F. Bertsch, Phys. Rev. C **44**, 2095 (1991).
5. B.A. Li, Nucl. Phys. A in print (1993).
6. H.R. Schmidt *at al.* (WA-80 collaboration), Nucl. Phys. A**544** 449c (1992).

MULTI-PION SYMMETRIZATION FOR RELATIVISTIC COLLISIONS

Scott Pratt

Ultra-relativistic heavy-ion collisions can produce hundreds of pions in a single event. The Bose-Einstein nature of the pions affects the multiplicity distribution, the singles spectra and the two-body correlation function. For instance, given a source much larger than the thermal wavelength, identical-particle statistics change the single-particle spectra from the Boltzmann distribution to the Bose-Einstein distribution. Two-particle emission is enhanced for pions with nearly the same momentum, a property used in two-particle correlation measurements to infer source size and collision dynamics. However, both one and two-body measurements are affected by the requirement that the entire n-body wave function needs to be symmetrized. Reference 1 had carefully studied methods for calculating these sort of effects with Monte Carlo methods. Unfortunately, these techniques were computationally intensive, making it difficult to explore the various physical aspects. We have developed a diagrammatic method which allows rapid calculation of Bose Einstein enhancements to all orders for a finite system [2]. We were even able to find analytic expressions for the case of a thermal source with a gaussian geometry.

We explored symmetrization corrections to multiplicity distributions by assuming a source which would yield a Poissonian multiplicity distribution with a mean η in the absence of symmetrization effects. Symmetrization weights the high multiplicity events more strongly. The figure below shows how the resulting average multiplicity depends on η for a gaussian source of $R = 1.5fm$ thermally emitting with a p_T of 313 MeV.

For any η that exceeds a critical value η_c, the resulting pion multiplicity is infinite. This represents the laser threshold, where the induced emission, in turn, induces more emission until all sources emit pions into a low momentum state. For large sources this occurs when the phase space filling factor exceeds unity for some region of phase space. This might be the case for the lead beam at CERN which is scheduled for 1994.

The laser-like behavior clearly manifested itself in the single-body spectra which showed a dramatic peak for the low momentum states. The two-body correlation functions were also affected by multi-body effects. For possonian emitters, the correlation function broadened beyond the usual $1/R$. If one however constructed the correlation function from events of fixed multiplicity the behavior was quite different. The intercept then fell sharply for multiplicities much higher than η_c. This was due to the fact that if all the pions are in the condensate and have the same momentum, they can not enhance others to have the same momentum any more than they already have the same momentum as evidenced by the singles spectra.

The isospin distributions are affected as well. Symmetrization enhances the probability that the emitted pions will be of the same flavor. This sort of behavior has been seen in cosmic rays known as Centauro events [3]. Reference 2 demonstrates how if a large number of pions comes from a source of hadronic size, or slightly larger, large isospin fluctuations occur due to symmetrization alone.

Now that the calculation of multi-body effects have become much more tractable, and observing laser-like behavior appears possible, we are working to study symmetrization effects in context of more realistic theoretical descriptions.

References

1. W.A. Zajc, Phys. Rev. **D35** 3396 (1987).
2. S. Pratt, "Pion Lasers for High Energy Collisions", to appear in Physics Letters **B**.
3. C.M.G. Lattes,Y. Fujimoto, S. Hasegawa, Phys. Rep. **65**.

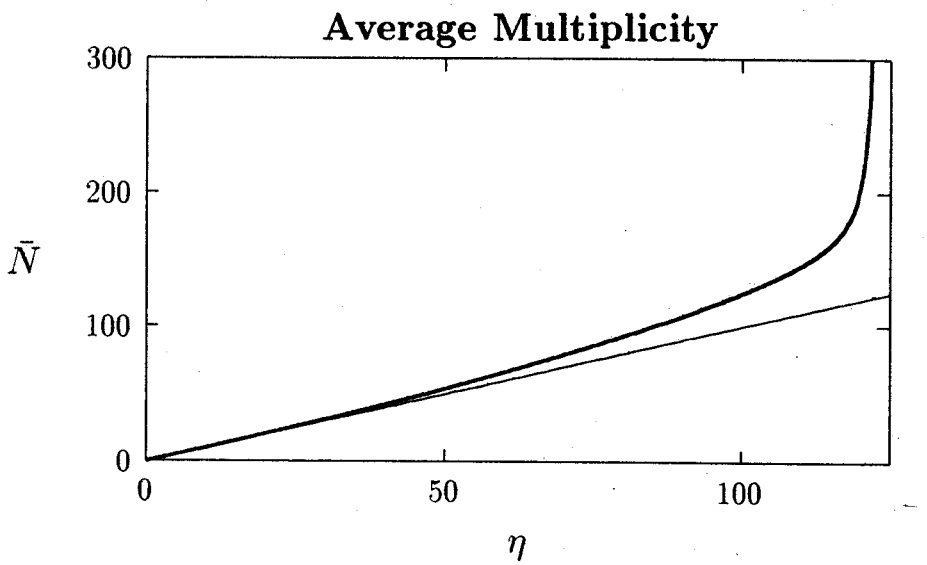

Figure 1: The heavy line represents the mean multiplicity for a system that would emit with Poissonian weights characterized by η, if symmetrization were neglected. The source function was assumed to be gaussian with $R = 3.5fm$. As η approaches η_c the average multiplicity goes to infinity. If the source were large, symmetrization would not be important and the result would be the light line, $\bar{N} = \eta$.

SIMPLIFIED TREATMENT OF STATISTICAL EMISSION

Brett V. Carlson[a]

Statistical emission from a compound nucleus is one of the best studied of all nuclear reactions. A quantum-mechanically consistent description of the process was developed in the early 50's by Hauser and Feshbach.[1] The success of this description is indisputable.

Calculations of multiple emission within the Hauser-Feshbach model can be quite cumbersome and time consuming, however. The aim of this work is to simplify the numerical calculations required of the model without sacrificing its fairly precise description of compound nucleus decay. One effort in this direction, by Friedman and Lynch,[2] has proven quite successful at describing the yields of particles emitted from highly excited nuclei. As their model describes the decay process in terms of an average compound nucleus, it cannot describe the distribution of evaporation residues remaining afterwards.

The initial objective of this work was to extend the Friedman-Lynch model to permit the calculation of evaporation residue yields. Many extensions and approximations were tested before a reasonable solution was found. To obtain a good description of the distribution of evaporation residues, it was necessary to treat explicitly the charge, mass and excitation energy of the compound nucleus. Only the angular momentum lent itself to a treatment in terms of its average value and the width of its distribution.

A typical statistical emission code, such as CASCADE,[3] calculates the residual populations, in excitation energy and angular momentum, for each type of particle emission from each compound nucleus in the decay chain. The simplified treatment also calculates the emission of each particle type from each compound nucleus. But it follows the decay chain initiated by one partial wave alone, calculating the spin-summed population and average value of the angular momentum and the width of its distribution for each residual. The restriction to a single initial partial wave permits simplifications and approximations to the calculation of transitions along the decay chain that compensate the sum over initial angular momenta that must be performed in the end. Calculations based on the simplified treatment run in about the same time as CASCADE calculations but use much less memory. Results of the two show quite good agreement.

The simplified treatment is easily extended to permit the emission of many particle types. It has been used with success in an analysis of data in which the emission of n, p, d, t, ^3He and α was taken into account.[4] Its extension to permit the emission of complex (excited) nuclei is now being studied.

a. Permanent Address: Instituo de Estudos Avançados, Centro Técnico Aeroespacial, 12231 São José dos Campos SP, Brazil

References

1. W. Hauser and H. Feshbach, Phys. Rev. **87** (1952) 366
2. W. A. Friedman and W. G. Lynch, Phys. Rev. **C28** (1983) 16.
3. F. Pühlhofer, Nucl. Phys. **A280** (1977) 267.
4. A. Szanto de Toledo et al., Phys. Rev. Lett. **70** (1993) 2070

ABRASION-ABLATION APPROACH TO PROJECTILE FRAGMENTATION

Brett V. Carlson[a]

Early models of projectile fragmentation assumed that the process occurs in two stages: a violent abrasive one, in which a primary fragment is formed of the nucleons which do *not* collide, and a subsequent ablation stage, in which the excited primary fragment decays.[1,2,3] A basic difficulty of these models was their estimate of the excitation energy deposited in the primary fragment by the abrasion process.

Two recent works have returned to abrasion-ablation type models to try once more to obtain a simple description of the observed experimental yields.[4,5] They approximate the primary fragment excitation energy, ϵ, as that of the holes left by the abraded nucleons. The agreement of these models with the data is surprisingly good, given the importance of secondary collisions that they do not include. The goal of this work is to calculate such abrasion-ablation yields as precisely as possible.

Beginning with the Glauber approximation to heavy-ion scattering cross sections and

- summing over unobserved final states,
- using antisymmetry and closure to simplify,
- using the coherent approximation to the average over the initial target state[3] and
- neglecting cross-terms containing the overlap of distinct single particle states,

one can reduce the expression for the differential primary yield to a sum over all combinations of single particle occupation probabilities with the desired charge and mass,

$$\frac{d\sigma_0}{d\epsilon}(\epsilon, Z_f, A_f) = \sum_{occ,nocc} \omega(\epsilon; occ, nocc) \times$$

$$\int d^2b \prod_{\pi_i \in occ} P_{\pi_i}(\vec{b}) \prod_{\overline{\pi}_j \in nocc} (1 - P_{\overline{\pi}_j}(\vec{b})) \prod_{\nu_k \in occ} P_{\nu_k}(\vec{b}) \prod_{\overline{\nu}_l \in nocc} (1 - P_{\overline{\nu}_l}(\vec{b})).$$

where *occ* and *nocc* represent the sets of occupied and unoccupied orbitals of each configuration, respectively.

The geometry of the abrasion process is contained in the impact parameter integral. The probability that the projectile proton in the state π_i passes through the target without colliding is

$$P_{\pi_i}(\vec{b}) = \left| \int d^2s dz \; |u_{\pi_i}(z, \vec{s})|^2 \, e^{-i\frac{m}{\hbar^2 k} \int dz \, U_\pi(z, \vec{b}-\vec{s})} \right|^2,$$

where U_π is the proton-target optical potential. This expression can be simplified somewhat by using the impulse approximation to the potential,

$$i\frac{m}{\hbar^2 k} U_\pi(z, \vec{b} - \vec{s}) = 0.5\sigma_{pp}\rho_\pi^T(z, \vec{b} - \vec{s}) + 0.5\sigma_{pn}\rho_\nu^T(z, \vec{b} - \vec{s}),$$

where σ_{pp}, σ_{pn} and $\rho^T_{\pi,\nu}$ are proton-proton and proton-neutron total cross sections and the target proton and neutron densities, respectively. The neutron probabilities, $P_{\nu_k}(\vec{b})$, can be expressed similarly.

The density of excited primary fragment states, $\omega(\epsilon; occ, nocc)$, relates the particle-hole configuration of the projectile fragment to its excitation energy. It is approximated by the density of hole states left by the abraded nucleons.

The particle evaporation of the ablation stage is calculated in the Weisskopf-Ewing approximation, which neglects angular momentum conservation. When the result is written as the probability, $P(Z, A; \epsilon, Z_f, A_f)$, of yielding a residue (Z, A), given a primary fragment (Z_f, A_f) with excitation energy ϵ, the observed secondary yield, $\sigma(Z, A)$, takes the form

$$\sigma(Z,A) = \sum_{Z_f,A_f} \int d\epsilon\, P(Z,A;\epsilon,Z_f,A_f) \frac{d\sigma_0}{d\epsilon}(\epsilon, Z_f, A_f).$$

Initial calculations confirm the success of the simpler models, at least in the case of light nuclei. A systematic study is now in progress.

a. Permanent Address: Instituto de Estudos Avançados, Centro Técnico Aeroespacial, 12231 São José dos Campos SP, Brazil

References

1. R. Serber, Phys. Rev. **72** (1947) 1114.
2. J. D. Bowman, W. J. Swiatecki and C. F. Tsang, LBL Report LBL-2908, 1973 (unpublished).
3. J. Hüfner, K. Schäfer and B. Schürmann, Phys. Rev. **C12** (1975) 1888.
4. J. J. Gaimard and K. H. Schmidt, Nucl. Phys. **A531** (1991) 709.
5. B. V. Carlson, M. S. Hussein and R. C. Mastroleo, Phys. Rev. **C46** (1992) R30.

MEAN FIELD OUT OF CHAOS

V. Zelevinsky

The concept of mean field (MF) plays a fundamental role in quantum many-body theory being a unique base for practically all microscopic calculations. Here we consider this notion from a non-standard point of view, namely we show that if one assumes the existence of extremely complicated quasichaotic dynamics, the average over the ensemble of the typical wave functions around given energy leads to the MF-description.

The derivation uses the exact operator equations of motion for the generalized density matrix [1] which is nothing but the complete set of matrix elements of particle-hole operator $a_1 a_2^\dagger$ in the Hilbert space of a system. In the nonlinear term we take the average over complicated intermediate states. The averaging procedure turns out to be almost determined by the strict requirements of quantum statistics and by the invariance under phase transformation of the wave functions. This results in the MF-type equations which differ from the conventional Hartree-Fock ones in taking into account the fluctuations of occupation numbers.

Since the MF is shown to be the smooth component of many-body dynamics which survives the averaging over complicated individual wave functions, it provides us with the optimum separation of global behavior from the local fluctuations which can be described with the aid of random matrix theory. Therefore it solves the longstanding problem of the most appropriate ("natural") basis which should be used in evaluating the degree of complexity of chaotic wave functions.

The next step in the development of the theory has to be connected with the analysis of collective modes, especially soft modes responsible for the instability of the MF and phase transitions.

References

1. V.G.Zelevinsky, Prog. Theor. Phys. Suppl. **74-75** (1983) 251.

FROM SIDEWARD FLOW TO NUCLEAR COMPRESSIBILITY

Qiubao Pan and Pawel Danielewicz

The purpose of this report is to show that differences between experiments investigating the dependence of sideward flow on multiplicity [1,2] can be exploited in a transport description to assess, independently, the effects of momentum and density dependence of the optical potential on the flow. A prime source of uncertainty in the determination of nuclear compressibility becomes, in consequence, uncertainty in the NN cross sections.

Our transport model of heavy-ion collisions is based on a set of equations [3] for nucleons, nucleon resonances, and pions.

$$\frac{\partial f_a}{\partial t} + \frac{\partial \mathcal{E}_a}{\partial \mathbf{p}_a}\cdot\frac{\partial f_a}{\partial \mathbf{x}} - \frac{\partial \mathcal{E}_a}{\partial \mathbf{x}}\cdot\frac{\partial f_a}{\partial \mathbf{p}_a} = \mathcal{K}_a^<(1\mp f_a) - \mathcal{K}_a^> f_a, \tag{1}$$

where f_a is the Wigner function. $\mathcal{E}_a$ is energy, and $\mathcal{K}_a^<$ and $\mathcal{K}_a^>$ are, respectively, the production and absorption rates of the particle a. An optical potential in the baryon energies is parametrized in a local frame where the spatial component of the baryon 4-vector current,

$$j^\mu = (\rho, \mathbf{j}) = \sum_a (\rho_a, \mathbf{j}_a) = \sum_a \left(\frac{g_a}{(2\pi)^3}\int d^3p_a\, f_a, \frac{g_a}{(2\pi)^3}\int d^3p_a \frac{\partial \mathcal{E}_a}{\partial \mathbf{p}_a} f_a \right), \tag{2}$$

vanishes. The factor g_a is spin degeneracy. Covariance of (2) may be verified by a direct calculation. The potential parametrization is similar to that in nonrelativistic calculations [4].

$$\begin{aligned} U_a &= \mathcal{A}\frac{\rho}{\rho_0} + \mathcal{B}\left(\frac{\rho}{\rho_0}\right)^\gamma + \frac{\mathcal{C}}{\rho_0}\sum_b \frac{g_b}{(2\pi)^3}\int d^3p_b \frac{f_b}{1+\left(\frac{p_b}{\Lambda}\right)^2} \\ &\quad + \mathcal{C}\frac{\rho}{\rho_0}\frac{1}{1+\left(\frac{p_a}{\Lambda}\right)^2} + t_3^a \frac{\mathcal{D}}{\rho_0}\sum_b t_3^b \rho_b. \end{aligned} \tag{3}$$

where t_3^a is the third component of isospin of the particle a. Equations (1) are solved for different values of the parameters in (3), with U treated as the fourth component of a vector potential, added to particle energy in a local frame. In tests we see no appreciable difference in our results when treating U as a scalar potential, added to mass, for the same parameter values.

Parameters in (3) are constrained by requiring that the energy per nucleon in cold symmetric matter has a minimum of $E/A \simeq$ -16 MeV at $\rho_0 \simeq 0.145$ fm^{-3}. The four different sets of parameters, two momentum dependent ones (C$\neq$0) and two non-momentum dependent ones, are listed in the following table.

EOS	Symbol	U(p=∞)(MeV)	A(MeV)	B(MeV)	γ	C(MeV)	Λ(MeV)	K(MeV)
Soft	S	-	-348	298	1.667	0	-	199
Hard	H	-	-119	68.5	2.0	0	-	371
Soft p-dep.	SM	0	362	-305	0.9	-71	400	176
Hard p-dep.	HM	35	76.4	51.7	1.9	-104	550	323

The factor in the isospin term in (3) is set equal to $\mathcal{D} = 92$ MeV, in order to reproduce the asymmetry coefficient in the binding-energy formula. For more details on our approach see Ref. [3].

Let us now turn to data. In Figs. 1 (a) and (b) we show (filled squares) the values of the flow parameter F from the measurements at 400 MeV/nucleon of the Nb + Nb reaction by the Plastic Ball Group [1], and of the Ar + Pb reaction by the DIOGENE Collaboration [2]. The parameter F is defined in our work as [2]

$$F = \left. \frac{d\langle p^x/m \rangle}{dy} \right|_{y_0}, \tag{4}$$

where p^x is the transverse momentum component in the reaction plane. The average is taken at a fixed rapidity y, and y_0 is the rapidity of intercept, $\langle p^x/m \rangle(y_0) = 0$. For the Nb + Nb reaction the flow parameter is presented as a function of the participant proton multiplicity N_p, and for the Ar + Pb reaction it is presented as a function of the impact parameter b estimated in the experiment. Of importance for subsequent considerations

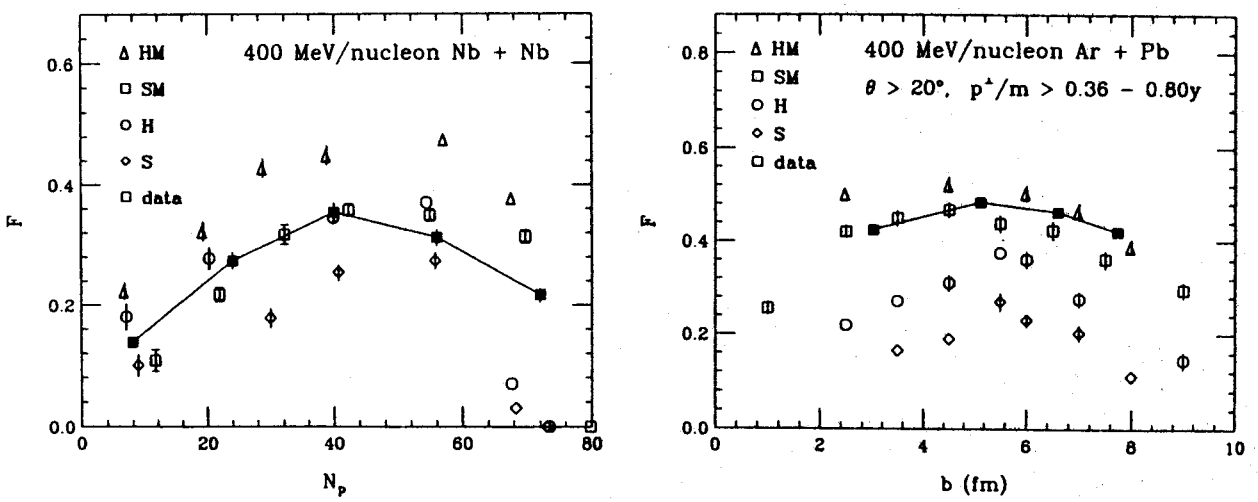

Figure 1: a) Flow parameter F in Nb + Nb reactions at 400 MeV/nucleon. Data of reference 1 (filled squares) are compared to the results of calculations for different optical potentials (open symbols). The abscissa shows participant proton multiplicity. Error bars for the results of calculations, suppressed when less than symbol size, represent uncertainties due to finite statistics. b) Similar to (a), except it is for the Ar + Pb reaction at 400 MeV/nucleon and the abscissa shows impact parameter.

are acceptances in the experiments. The combined Plastic Ball and Wall detectors have good acceptance [1] for protons emitted in the forward laboratory direction with velocities above $0.3c$. Experimenters provide a filter program that simulates the acceptance. Data of Ref. [2] are subjected to software cuts which eliminate, in the forward direction, the particles emitted under an angle of 20° and, further, those particles whose transverse momenta satisfy $p^{\perp}/m < 0.36 - 0.80y$.

Besides the results of measurements, we show in Figs. 1 the results of our transport-model calculations (open symbols) for the different optical potentials, with emitted protons subjected to the acceptance filters. It is seen in Figs. 1,

that calculations utilizing potential S generally underpredict the measured flow values, the calculations utilizing potential H quite clearly underpredict measured values in Ar + Pb reaction, while those utilizing

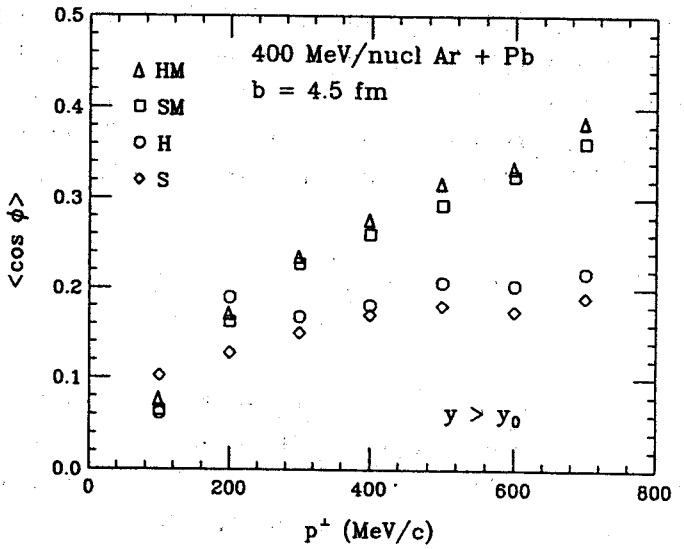

Figure 2: Mean cosine of the azimuthal angle, with respect to the reaction plane, of nucleons emitted at $y > y_0$, as a function of the nucleon transverse momentum.

potential HM overpredict the flow values in Nb + Nb reaction. Only calculations utilizing potential SM conform, to a reasonable extent, with data for either of the reactions.

The differences between the predictions of calculations utilizing SM and H potentials, present at all b in Ar + Pb reaction, are startling, just as startling is the failure of calculations utilizing potential H to reproduce data. In past studies [4-6], and for the Nb + Nb reaction, the two types of potential gave similar results for same b. While some differences between the predictions for the Ar + Pb reaction are present prior to the application of acceptance cuts (predictions based on two types of potentials were never compared for strongly asymmetric systems), the differences are more than doubled by the cuts. The effect may be understood by examining Fig. 2. In this figure we show, as a function of transverse momentum, the average values of cosine of the azimuthal angle with respect to reaction plane, of nucleons emitted at $y > y_0$ from $b = 4.5$ fm reaction, for the different potentials. It is seen that particles with high $p^{\perp}$ are much more focussed at one side of the beam axis in the vicinity of the reaction plane for momentum-dependent than for momentum-independent potentials. Indeed, in the case of a momentum-dependent potential, the particles with high momenta are subjected to an enhanced repulsion in the central region of a reaction. When an analysis is limited to particles emitted with high $p^{\perp}$, the flow values for a potential dependent on momentum rise relative to the flow values for a momentum-independent potential. Predictions based on the SM potential agree to a reasonable extent with the DIOGENE data on the variation of flow with b in the Ne+Pb reaction at 800 MeV/nucleon and also with the Steamer Chamber data on the variation of $< p^x/A >$ with y in the semicentral Ar+Pb events at that bombarding energy. In Fig. 3, a good agreement can be seen between the calculated and measured flow values at several bombarding energies in the Nb + Nb reaction, at a fixed reduced multiplicity [1]. Other systems where consistency between the SM predictions and data was found include Au + Au and Ca + Ca at 400 MeV/nucleon [1].

It is important to consider an effect on the conclusions concerning K, of the possible reduction of cross sections in the medium. A comparison of the calculated and measured rapidity distributions in the reactions at 400 and 800 MeV/nucleon [9,8], excludes an overall reduction of the elementary cross sections by more than $\sim 35\%$ relative to free space at the high energies, but not by a lesser amount. An effect of the 35% reduction on the flow parameter in calculations utilizing the SM potential, is illustrated in Fig. 3. An acceptable agreement with the Nb + Nb and Ar + Pb data, for the reduced cross sections, is obtained when K is raised to 205 MeV,

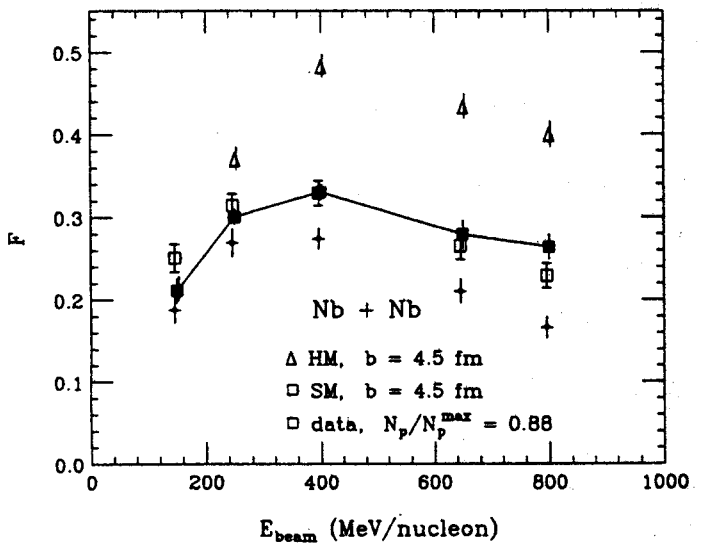

Figure 3: Flow parameter in the Nb + Nb reaction as a function of beam energy. Experimental values (filled squares) for the fourth bin of reduced multiplicity [2], $N_p/N_p^{max} \simeq 0.88$, are compared to the results of calculations at $b = 4.5$ fm for HM potential (open triangles), SM potential (open squares), and SM potential and the cross sections reduced by 35% (crosses).

with potential parameters following from such constraints as before. Using the behavior of our predictions with K, m^*, and cross sections, and the actual deviations of the SM predictions from data, and further taking into account some uncertainty associated with the form of a potential, we estimate that nuclear compressibility lies between 165 and 220 MeV.

References

1. H. Å. Gustafsson *et al.*, Mod. Phys. Lett. A **3**, 1323 (1988).
2. M. Demoulins, Ph. D. Thesis, University Paris Sud, 1989 [Report CEA-N-2628, CEN Saclay, 1990]; J. Gosset *et al.*, in *The Nuclear Equation of State*, edited by W. Greiner and H. Stöcker, NATO ASI Series (Plenum, N.Y., 1989) Vol. 216A, p.87; M. Demoulins *et al.*, Phys. Lett. B **241**, 476 (1990).
3. P. Danielewicz and G.F. Bertsch, Nucl. Phys. **A533**, 712 (1991).
4. C. Gale *et al.*, Phys. Rev. C **35**, 1666 (1987).
5. J. Aichelin *et al.*, Phys. Rev. Lett. **58**, 1926 (1987).
6. C. Gale *et al.*, Phys. Rev. C **41**, 1545 (1990).
7. P. Danielewicz and Q. Pan, Phys. Rev. C **46**, 2002 (1992).
8. D. Beavis *et al.*, Phys. Rev. C **45**, 299 (1992).
9. H. H. Gutbrod *et al.*, Z. Phys. **A337**, 57 (1990).

BLAST OF LIGHT FRAGMENTS FROM CENTRAL HEAVY-ION COLLISIONS

Paweł Danielewicz and Qiubao Pan

We study the effects of collective expansion on light fragment emission from central heavy-ion collisions by carrying out calculations in a transport model with dynamic production of $A \leq 3$ fragments [1]. The basis of the model is the set of coupled equations

$$\frac{\partial f_a}{\partial t} + \frac{\partial \mathcal{E}_a}{\partial \mathbf{p}_a}\cdot\frac{\partial f_a}{\partial \mathbf{x}} - \frac{\partial \mathcal{E}_a}{\partial \mathbf{x}}\cdot\frac{\partial f_a}{\partial \mathbf{p}_a} = \mathcal{K}_a^<(1 \mp f_a) - \mathcal{K}_a^> f_a, \tag{1}$$

where f_a is the Wigner function, and $\mathcal{K}_a^<$ and $\mathcal{K}_a^>$ are, respectively, the production and absorption rates of the particle a. Deuterons are produced in the interaction of three nucleons [2], while tritons and helions in the interaction of four nucleons. The processes of production and breakup are related by time reversal.

In the simulations of the central symmetric collisions of heavy nuclei, at beam energies of a few hundred MeV/nucleon [1], we observe a formation of the region with a dense excited nuclear matter that expands predominantly in the sideward directions, cf. Fig. 1. The expansion is reflected in the angular distributions

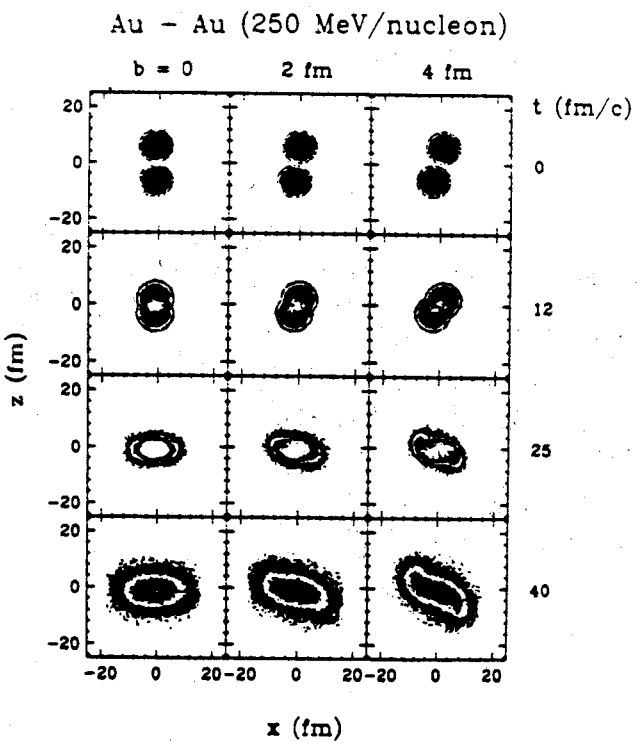

Figure 1: Contour plots of particle density integrated over the normal to reaction plane in Au+Au collisions at 250 MeV/nucleon.

and in the mean transverse energies of emitted fragments. At the late stage of the expansion the characteristic

features of local thermodynamic equilibrium are identified. Different particles share the same thermal energy and are further subject to the same collective-velocity field. Correspondingly, the mean particle energies rise linearly with the particle mass, e.g. the energies of particles at 90° degrees in the center of mass,

$$< E >_{90°} \simeq \frac{3}{2}\frac{m < v_\perp^2 >}{2} + \frac{3}{2}T = \frac{3}{2}A\frac{m_N < v_\perp^2 >}{2} + \frac{3}{2}T = \frac{3}{2}AE_{\perp N}^{coll} + \frac{3}{2}T. \quad (2)$$

The strength of the transverse collective motion and the rise of transverse energies depends on the bombarding energy and varying impact parameter in the collisions. In addition to the differences due to collective expansion in the transverse energies of particles with different mass, differences arise in the energies of particles with different charge due to Coulomb interactions as the particles move away from the reaction region. When comparing our results to data [3], consistency is found for the proton and helion energies, but not for the triton and deuteron energies, see Fig. 2. The results for the azimuthal distributions with respect to the reaction plane [1], with the anisotropies increasing with particle mass, are consistent with the measurements [4]. New data sets are analyzed right now, hopefully shedding more light on the situation.

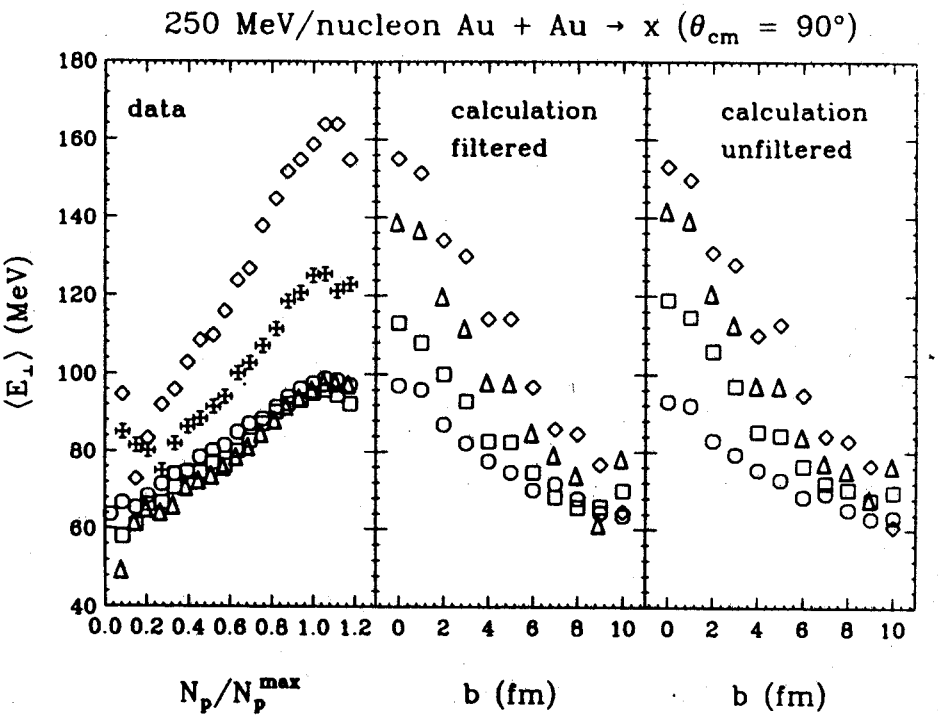

Figure 2: Mean kinetic energies of protons (circles), deuterons (squares), tritons (triangles), helions (diamonds), and alphas (crosses) in the Au+Au collisions at 250 MeV/nucleon. Left panel displays energies determined in the experiment of Ref. [3] . Center and right panels show the results of our calculation [1] as a function impact parameter in the direct form, and with the final state subjected to the procedure simulating detector acceptance, respectively.

References

1. P. Danielewicz and Q. Pan, Phys. Rev. C **46**, 2002 (1992).

2. P. Danielewicz and G. F. Bertsch, Nucl. Phys. **A533**, 712 (1991).
3. K. G. R. Doss, H. Å. Gustafsson, H. H. Gutbrod, K. H. Kampert, B. Kolb, H. Löhner, B. Ludewigt, A. M. Poskanzer, H. G. Ritter, and H. R. Schmidt, Mod. Phys. Lett. A **3**, 849 (1988).
4. H. H. Gutbrod, K. H. Kampert, B. Kolb, A. M. Poskanzer, H. G. Ritter, and H. R. Schmidt, Phys. Lett. B **216**, 267 (1989); H. H. Gutbrod, K. H. Kampert, B. Kolb, A. M. Poskanzer, H. G. Ritter, R. Schicker, and H. R. Schmidt, Phys. Rev. C **42**, 640 (1990).

OCTET BARYONS AT FINITE TEMPERATURE: QCD SUM RULES vs. CHIRAL SYMMETRY

Y. Koike

There has been an increasing amount of interest in the property change of hadrons at finite temperature in connection with the relativistic heavy ion collisions such as RHIC and LHC. In this work we studied the behavior of the octet baryon correlators at finite temperature in the framework of the QCD sum rule.[1] (For meson properties, see refs. 2, 3) At low temperature ($T \leq 150$ MeV) in the confined phase of QCD, the finite temperature medium can be well approximated by a noninteracting Goldstone boson (pion) gas. In this approximation, the condensates appearing in the OPE side of the correlators become T-dependent through the interaction with thermal pions. However, the $\pi + B \rightarrow B'$ scattering terms have to be consistently taken into account as a new structure in the phenomenological spectral functions. We showed that the $O(T^2)$-dependence of the condensates is completely compensated by the change of the pole residue and the above scattering effect. Therefore the baryon masses are constant to this order, although $\langle \bar{u}u \rangle_T \simeq \langle \bar{u}u \rangle (1 - T^2/8f_\pi^2)$, which is consistent with the chiral symmetry constraint by Leutwyler and Smilga. The pole residue for the nucleon decreases as $\lambda_N(T) \simeq \lambda_N(0)\{1 - (1 + g_A^2)T^2/32f_\pi^2\}$, and probably becomes zero at the phase transition point. The situation is analogous for other octet baryons.

In an earlier work [4], the nucleon mass at finite T was studied in a framework of the QCD sum rule. They erroneously observed a decreasing nucleon mass as the chiral order parameter decreases at finite T. In that work, the $\pi + B \rightarrow B'$ scattering term was not taken into account. They did not treat the T-dependence of all the condensates correctly, either. The present study shows that to study $O(T^4)$ or higher order effects with respect to T, we need to pay particular attention to the consistency between the OPE side and the form of the phenomenological spectral function.

References

1. Y. Koike, "Octet Baryons at Finite Temperature: QCD Sum Rules vs. Chiral Symmetry", MSUCL-870, January, 1993. Submitted to Nucl. Phys. **B**. /item Y. Koike, "Hadrons at Finite Temperature from QCD Sum Rules", Invited talk presented at "XI International Seminar on High Energy Physics Problems", Dubna, Russia, September 7-12, 1992. To be published in the proceedings. /item T. Hatsuda, Y. Koike and S.H. Lee, U of MD #92-203 (July, 1992), Nucl. Phys. **B** in press. U of MD #93-008 (July, 1992), Phys. Rev. **D** in press.
2. C. Adami and I. Zahed, Phys. Rev. **D45** (1992) 4312.

TWIST-4 MATRIX ELEMENTS OF THE NUCLEON FROM THE LATEST ANALYSIS OF CERN AND SLAC DIS DATA

Y. Koike, T. Hatsuda[a], S.H. Lee[a] and S. Choi[b]

Recent precision analysis of the lepton-nucleon deep inelastic scattering (DIS) data at CERN and SLAC in the broad kinematic region provides us with rich information about the nucleon structure functions. The spin-averaged DIS structure function can be schematically written as

$$A\,(\ln Q^2) + \frac{1}{Q^2} B(\ln Q^2) + \cdots, \tag{1}$$

where A and B are the twist-2 and 4 contributions, respectively, and each of them depends on the square of the virtual photon momentum Q^2 at most logarithmically. The A-term corresponds to the parton model and the B term describes quark-gluon or quark-quark correlations inside the nucleon. The combination of the old SLAC data (low Q^2) and the recent CERN data (BCDMS and NMC data at high Q^2) provides us some information about the nucleon matrix elements of the twist-4 operators which are related to the B term.

At this stage, the complete determination of all the twist-4 matrix elements from the experiments alone is impossible. We discussed what kind of constraint is required among these matrix elements, and how various nucleon models (diquark model, bag model etc) fail in describing the data. We found on a rather general physical assumption that the nucleon matrix element of the twist-4 quark-gluon mixed operator is relatively large compared with that of the four-quark operators. From the point of view of naive valence quark models, this is an unexpected situation.

a. Physics Department, FM-15, University of Washington, Seattle, WA 98195
b. Department of Physics, Yonsei University, Seoul 120-749, Korea

References

1. S.H. Lee, S. Choi, T. Hatsuda and Y. Koike, "Twist-4 Matrix Elements of the Nucleon from the Latest Analysis of CERN and SLAC DIS Data", February, 1993. Submitted to Phys. Lett. **B**.